NUMERICAL SIMULATION OF TURBULENT FLOW INSIDE AND AROUND COVERED ROADWAY

Mohamed Hefny*, Ryozo Ooka*
*The University of Tokyo, Tokyo, Japan

Abstract

The turbulent flow around covered roadway resembles an urban setting where pollutant concentrations exceed ambient air quality standards and exposure to large number of people exists as well. Numerical simulation of this type of flow is very important for understanding its behavior and characteristics. In this paper, the turbulent flow inside and around covered roadway is numerically simulated using non-linear k-ε model. The main objective of this study is to to provide some indications for the dynamics of the flow and to investigate the kinematics of vortex structures within and downwind of the covered section, also, to investigate the sensitivity of vortices to external conditions (i.e. aspect ratios, wind directions).

Key words: covered roadway, k-ε model, turbulent flow

1. INTRODUCTION

Covered roadways resembles a typical urban setting which characterized by high pollutant concentrations and exposure to large number of people. This urban setting is typically encountered in many places such as airports, bus terminals, parking structures and multi-level highways. In order to understand the structure of pollutant dispersion and transport, numerical as well as experimental investigations are needed.
Although this flow problem is quite common, few research publications reported this problem. Dabberdt et al.[1] have studied the transport and dispersion processes through wind tunnel experiments and numerical modeling. Their numerical simulations utilized k-ε turbulence closure. Afterwards, Laatar et al.[2] modeled the same problem using 2D large eddy simulation (LES) in order to see if 2D large eddy simulation could improve the discrepancies between the numerical and experimental results of Dabberdt et al.[1]. Then, Alexander and Dabberdt[3] evaluated the effect of two ventilation configurations air curtains, jets, and air pillars on peak and mean pollutant concentrations within the covered roadway.
The review of previous research reveals that the numerical simulations of this flow problem are not comprehensive in terms of modeling the kinematics and mass fields in and near this complex configuration. Also, the results of 2D large eddy simulation[2] are not reliable for similar applications which have 3D turbulence nature [4] in spite of its advantage of greatly reduced CPU time. This is confirmed specifically for this flow situation by comparing the 2D and 3D large eddy simulation in reference [5].
The scarce of comprehensive numerical simulations of this flow problem stimulated the authors to perform a series of numerical simulations in order to explore the kinematics of the vortex structures within and downwind of the covered section. In this paper, the first numerical modeling of this series is presented. The turbulent flow inside and around covered roadway is simulated using the Reynolds-averaged Navier–Stokes (RANS) equations. The non-linear turbulent k-ε model is used for the turbulence closure.

2. OUTLINE OF CFD COMPUTATIONS

In this computation, the flow filed around and inside covered roadway is considered for two cases; windward case and leeward case. In windward case, the open side is oriented downwind and perpendicular to the ambient flow, while in leeward case the open side is set perpendicular to the approaching flow as shown in Fig. 1.

3.1. Computational domain

The computational domain is chosen so that it covers 23h (streamwise direction), 7h (vertical direction) and 20h (lateral direction) where h is the height of the covered section. The choice of such dimensions is that it contains all the flow topologies and to satisfy the boundary conditions at the boundaries, see Fig. 1. The dimensions of the covered roadway are taken here analogous to the experiment performed by Dabberdt et al. [1], in which the covered section had a scaling ratio (model: full-scale) of 1:30. The corresponding full-scale height (h) is 3.81 m and two different widths (W) are used: 27.4 m and 13.7 m, resulting in width to height aspect ratios (α) of 7.2 and 3.6, respectively.

3.2. Computational mesh

Non-uniform meshes are used in which the computational domain is decomposed to hexahedral-based unstructured elements (1045216 control volumes in wide section case, i.e. α = 7.2, and 888376 control volumes in

narrow section, i.e. $\alpha = 3.6$). The mesh interval adjacent to the wall is 0.01*h* and the meshes are stretched in such way to better resolve regions of significant velocity gradients near the walls. The dimensions of the covered roadway are taken here analogous to the experiment done by Dabberdt et al[1].

3.3. Numerical and boundary conditions

The CFD code Star-CD®, based on the unstructured finite-control-volume discretization method, has been employed. All transport equations were discretized for at least second order accuracy in space. For the convective terms, a second order upwind scheme was used to interpolate values from cell centers to nodes. The diffusion terms were discretized using central differences. The nonlinear cubic k-ε model[6] was selected as the turbulent model in these simulations. The SIMPLE algorithm[7] was employed to evaluate pressure–velocity coupling.
At the inflow boundary, a velocity distribution in the stream-wise direction (u-velocity) is prescribed similar to the experiment of Dabberdt et al.[1] as $u = U(z/b)^{0.18}$ where U is the ambient velocity at a full scale height of 30 m while other velocity components (v and w) are set equal to zero. The turbulent kinetic energy, k, and the dissipation rate, ε, profiles are prescribed at the inlet according to:

$$k = 1.5(I \times U)^2 \,,\; I = 0.1 \,,$$

$$\varepsilon = C_\mu k^{3/2} / l \,,\; l = 4(C_\mu k)^{1/2} h^{1/4} Z^{3/4} / U$$

The generalized logarithmic law of the wall is applied to all solid boundaries (ground and covered section walls) while the outlet convective boundary condition is used at the downstream boundary [10]. For the sides of the computational domain, symmetry boundary conditions are prescribed whereas the top of the computational domain is modeled as a slip wall (zero normal velocity and zero normal gradients of all variables).

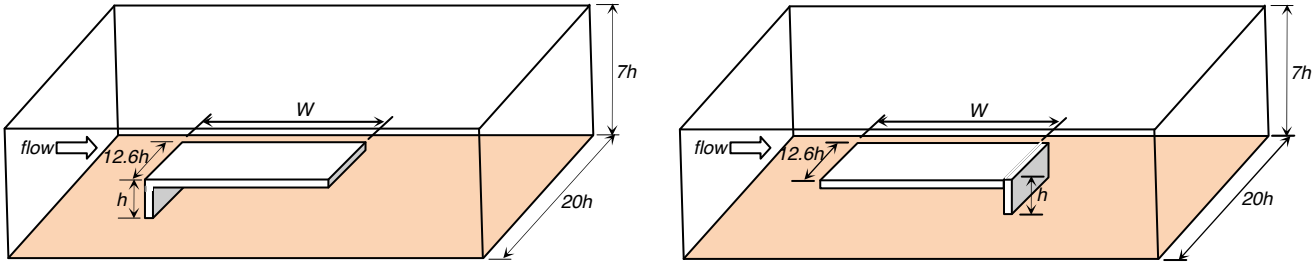

Figure 1: Computational domain for (a) leeward case and (b) windward case.

3. RESULTS

3.1. Model validation

The accuracy of the current simulations is validated with the wind tunnel measurements performed by Dabberdt et al.[1]. In the experiment, a neutrally buoyant gas mixture of ethane (C_2H_6) and air (the emission rate was 200 cm^3/min ethane in 1000 cm^3/min air) was used as the quantitative tracer. The tracer was released from a narrow line source 27.4 m long. Three test patterns were performed for leeward and windward cases to resemble three positions of the line source. Unfortunately, only the concentration measurements are available in the literature. Consequently, the concentration, not the velocity, profiles of the measurements and the simulation will be compared keeping in mind that some discrepancies are expected since RANS model is used in the simulations.
Normalized concentrations of pedestrian-level concentrations (C^*) from the wind tunnel experiments and the CFD simulations are illustrated in Fig. 2. for leeward case of aspect ratio α =7.2 for different three line source positions. Here the normalized concentration (C^*) is defined as $C^*=CU/q$ where C is the concentration, U is the ambient wind velocity, and q is the line source emission rate. The trend of the simulation profiles is consistent to the profile observed in the wind tunnel experiments. However, there are some differences in the details: the peak positions are shifted towards the line source section and the peak concentration values are higher than those of the experiments (1.4 times approximately).

3.2. Windward case

The dynamics of the flow inside and around the covered roadway in windward case can be demonstrated with the aid of Fig. 3 where the velocity vectors and the contours of u-component of the velocity are depicted. The values of u are normalized by the ambient velocity magnitude U. The flow is complex and its detailed topology is strongly affected by the size of the covered section. Figure 3 shows that the flow decelerates in front of the opened section then divides around the blocked section forming a pair of vortices behind the obstacle.

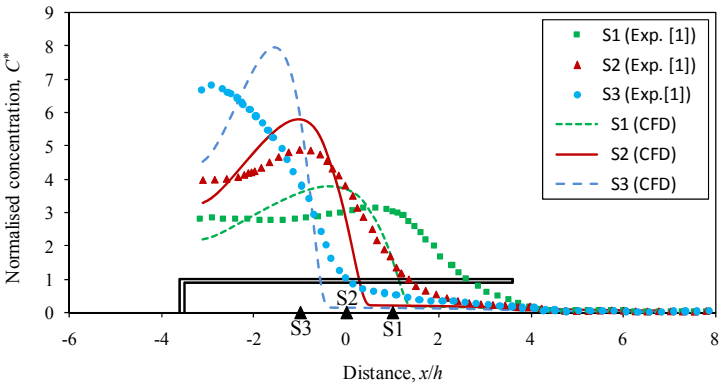

Figure 2: Measured and simulated profiles of pedestrian level concentrations for leeward case.

The size of the vortices depends upon the aspect ratio α. Above the covered section, the flow separates forming a vortex as shown in Figs. 3b and d. Although much weaker, the flow inside the covered section is also complex and a stagnant region in the vicinity of closed side is formed. The oncoming flow separates at the edge forming an interface region with strong velocity gradient which is expected to play important rule in the ventilation process inside the covered roadway.

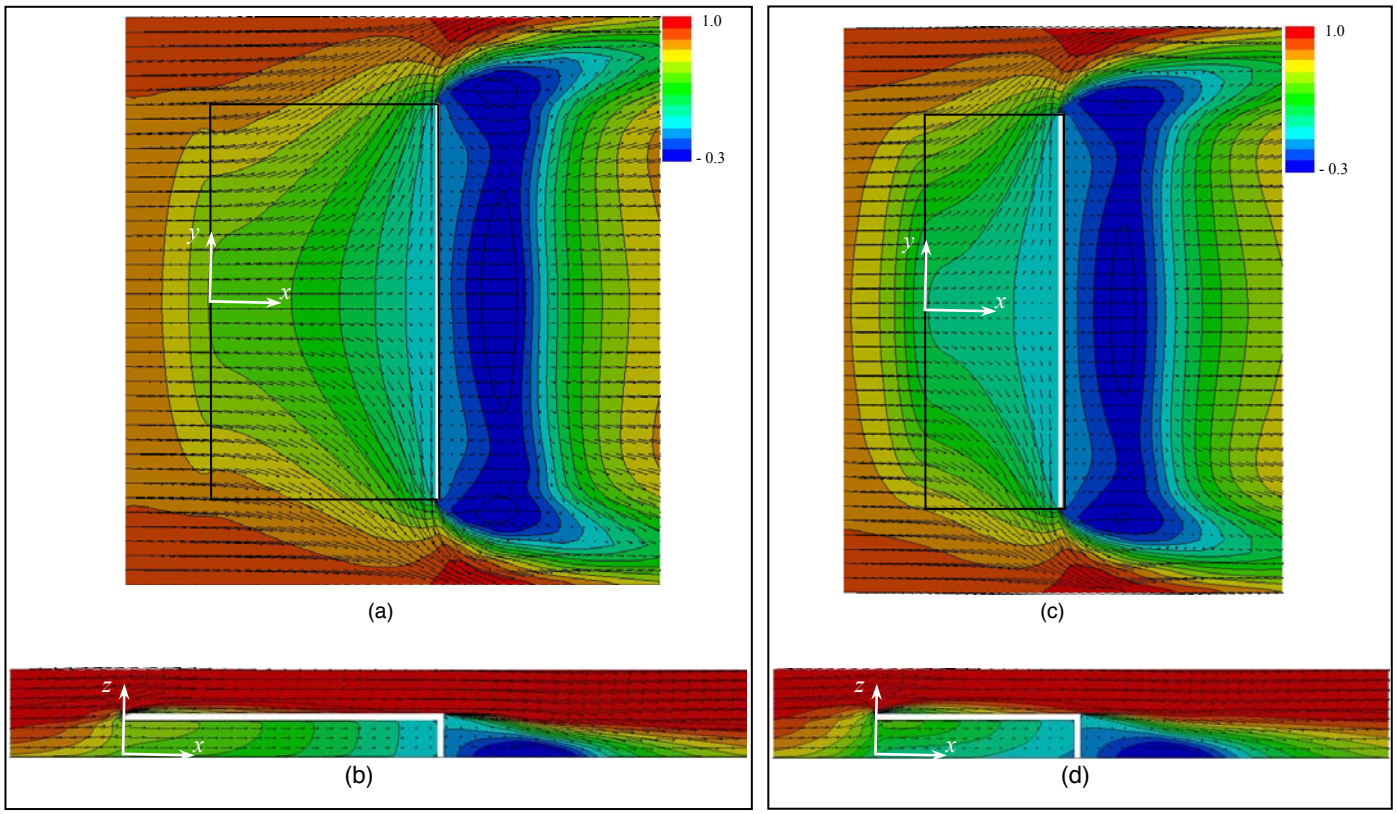

Figure 3: Velocity vectors and contours for windward case for (a,b) aspect ratio (α) =7.2 and (c,d) aspect ratio (α) =3.6.

3.3. Leeward case

When the open side is leeward, the expected strong interaction between the external and internal flows will result in much more unstable and turbulent flow, this can be seen clearly in Fig.4. The impinging flow on the closed side forms a vortex in front of the covered roadway. Then the flow separates on the corner above the covered section and reattached forming a vortex, similar to the bluff body situation. The flow then forms a wake vortex behind the covered section penetrating air deeply into the covered section. The size of this vortex, and hence the penetrating flow, depends upon the aspect ratio α. Inside the covered section, two counter-rotating vortices are formed, see

Figs. 4.a and c, and occupy most of the covered section. The interaction between those two vortices and the wake vortex is expected to govern the ventilation process inside the covered section. For instance, the wake vortex will stimulate some entrainment of fresh air and eventually ejects in air inside the covered section while the two counter-rotating vortices partially will carry the contamination out from the covered section.

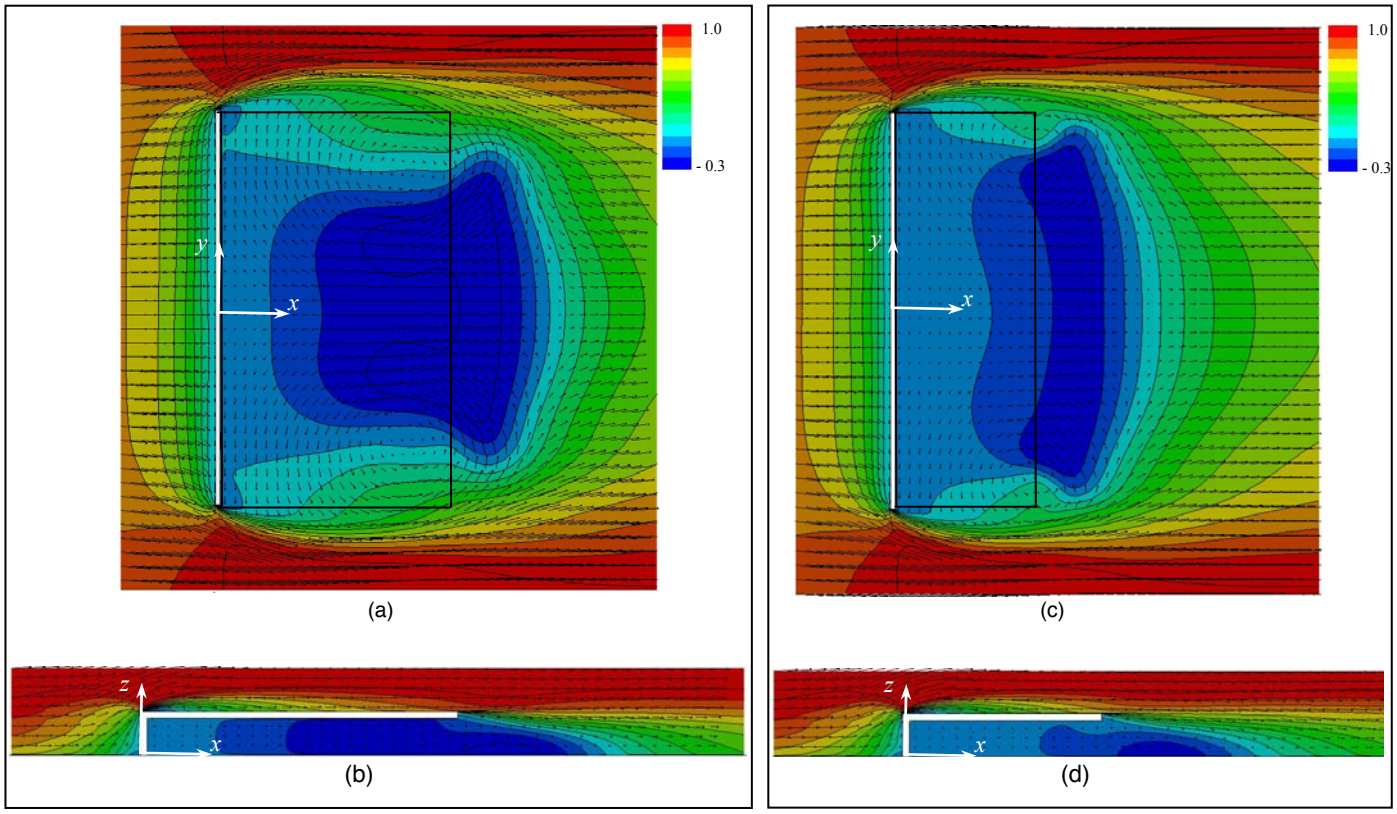

Figure 4: Velocity vectors and contours for leeward case for (a,b) aspect ratio (α) =7.2 and (c,d) aspect ratio (α) =3.6.

4. CONCLUSIONS

In this paper, the turbulent flow inside and around covered roadway is simulated using RANS model in which the non-linear turbulent k-ε model is used for the turbulence closure. The flow kinematics and the vortex structures within and downwind of the covered section is described in case of different external conditions of wind direction and aspect ratio of the covered section.

References

[1] Dabberdt, W.F., Hoydysh, W.G., Read, M., 1998. Pollution dispersion at complex street configurations: covered roadways, *International Journal of Vehicle Design*, 20 (1–4), 96-104.
[2] Laatar, A.H., Benahmed, M., Belghith, A., Le Quere, P., 2002. 2D large eddy simulation of pollutant dispersion around a covered roadway, *Journal of Wind Engineering and Industrial Aerodynamics*, 90 (6), 617-637.
[3] Alexander, L.B., Dabberdt, W.F., 2003, Modelling ventilation and dispersion for covered roadways, *Journal of Wind Engineering and Industrial Aerodynamics*, 91, 593-608.
[4] Murakami, S., Rodi, W., Mochida, A., Sakamoto, S., 1993. Large eddy simulation of turbulent vortex shedding flow past 2D square cylinders, *Engineering Applications of large eddy simulations*, 162, 113-120.
[5] Hefny, M.M., Ooka, R., 2008. Large eddy simulation of flow around covered roadway: comparison between 2D and 3D simulation, 日本流体力学会年会, 25144, 1-3.
[6] STAR-CD Version 3.22, 2004. STAR-CD Methodology, Computational Dynamics Limited.
[7] Patankar, S.V., Spalding, D.B, 1972. A calculation procedure for heat mass and momentum transfer in three-dimensional parabolic flows. Heat Mass Transfer, 15, 1787-1806.